ISBN: 978-3-95450-194-6 doi:10.18429/JACoW-LINAC2018-TUPO078

EXTENSION OF BUSCH'S THEOREM TO PARTICLE BEAMS

L. Groening[1], M. Chung[2], and C. Xiao[1]
[1]Gesellschaft für Schwerionenforschung, Darmstadt, Germany
[2]Ulsan National Institute of Science and Technology, Ulsan 44919, Republic of Korea

Abstract

In 1926, H. Busch formulated a theorem for one single charged particle moving along a region with longitudinal magnetic field. The theorem relates particle angular momentum to the amount of field lines being enclosed by the particle cyclotron motion. It has been extended to accelerated particle beams. This contribution sketches the extension and applies the extended theorem to successfully performed emittance manipulations with electron and ion beams.

BUSCH'S THEOREM FOR SINGLE PARTICLE

In 1926, H. Busch applied the preservation of angular momentum for systems with cylindrical symmetry to a charged particle moving inside a region with magnetic field $\vec{B}$ [1]. Using conjugated momenta, the magnetic field strength is intrinsically included into the equations of motion. In linear systems, the normalized conjugated momenta p_x and p_y are related to the derivatives of the particle position coordinates (x, y) w.r.t. the main longitudinal direction of motion $\vec{s}$ through

$$p_x := x' + \frac{\mathcal{A}_x}{(B\rho)} = x' - \frac{yB_s}{2(B\rho)}, \qquad (1)$$

$$p_y := y' + \frac{\mathcal{A}_y}{(B\rho)} = y' + \frac{xB_s}{2(B\rho)}, \qquad (2)$$

where $\vec{\mathcal{A}}$ is the magnetic vector potential with $\vec{B} = \vec{\nabla}\times\vec{\mathcal{A}}$, B_s is the longitudinal component of the magnetic field, and $(B\rho)$ is the particle rigidity, i.e., its momentum per charge $p/(qe)$, with p as total momentum, q as charge number, and e as elementary charge. Busch's theorem states that the canonical angular momentum $\tilde{l} = xp_y - yp_x$ is a constant of motion that is written in cylindrical coordinates as

$$m\gamma r^2\dot{\theta} + \frac{eq}{2\pi}\psi = const\,. \qquad (3)$$

A general formulation of Eq. (3) has been derived in [2], which is regarded as the generalized Busch theorem

$$\oint_C \vec{v}\cdot d\vec{C} + \frac{eq}{m\gamma}\psi = const\,, \qquad (4)$$

i.e., the path integral around a stream of possible particle trajectories along a closed contour C, plus the magnetic flux through the area enclosed by C is an invariant of the motion. Figure 1 illustrates the first part of the left hand side of Eq. (4). Busch's theorem of Eq. (3) is the special case of this generalized form for C being a circle of radius r. It is emphasized that Eq. (4) is only valid for laminar motion.

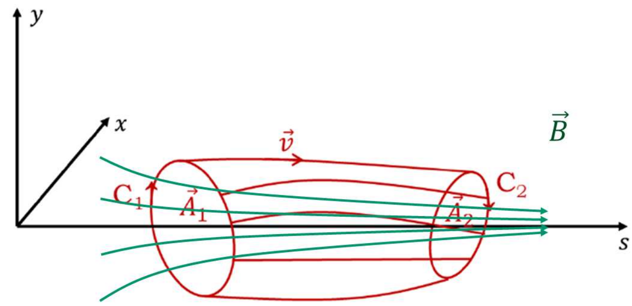

Figure 1: Fig. 3 from [3]: the contour C encloses possible streams of particle trajectories and encloses the area $\vec{A}$.

TRANSVERSE EIGEN EMITTANCES

The transverse eigen emittances were introduced by Dragt in 1992 [4] as the two transverse rms-emittances the beam acquires after all inter-plane correlations have been removed by appropriate linear beam line elements. They are calculated from the 2nd-moments beam matrix

$$\tilde{C} = \begin{bmatrix} \langle x^2\rangle & \langle xp_x\rangle & \langle xy\rangle & \langle xp_y\rangle \\ \langle xp_x\rangle & \langle p_x^2\rangle & \langle yp_x\rangle & \langle p_xp_y\rangle \\ \langle xy\rangle & \langle yp_x\rangle & \langle y^2\rangle & \langle yp_y\rangle \\ \langle xp_y\rangle & \langle p_xp_y\rangle & \langle yp_y\rangle & \langle p_y^2\rangle \end{bmatrix}, \qquad (5)$$

together with

$$J = \begin{bmatrix} 0 & 1 & 0 & 0 \\ -1 & 0 & 0 & 0 \\ 0 & 0 & 0 & 1 \\ 0 & 0 & -1 & 0 \end{bmatrix}. \qquad (6)$$

as [5]

$$\tilde{\varepsilon}_{1/2} = \frac{1}{2}\sqrt{-tr[(\tilde{C}J)^2] \pm \sqrt{tr^2[(\tilde{C}J)^2] - 16\,det(\tilde{C})}}\,. \qquad (7)$$

The product of the two eigen emittances is equal to the 4d rms-emittance $\tilde{\varepsilon}_{4d}$ being in turn equal to the square root of the determinant of $\tilde{C}$. By definition $\tilde{\varepsilon}_{1/2/4d}$ are preserved by linear beam line elements as drifts, quadrupoles, dipoles, and solenoids even if they are tilted.

PRESERVATION OF EIGEN EMITTANCES

Busch's theorem was obtained from expressing preservation of axial angular momentum using conjugate momenta. Its extension to beams is achieved in analogue way by ex-

ISBN: 978-3-95450-194-6 doi:10.18429/JACoW-LINAC2018-TUPO078

pressing the preservation of the sum

$$\tilde{\varepsilon}_1^2 + \tilde{\varepsilon}_2^2 = -\frac{1}{2} tr[(\tilde{C}J)^2] = \tilde{\varepsilon}_x^2 + \tilde{\varepsilon}_y^2 + 2\left(\langle xy\rangle\langle p_x p_y\rangle - \langle y p_x\rangle\langle x p_y\rangle\right) = const \tag{8}$$

using conjugate momenta as shown in detail in [3]. Substitution of the conjugate momenta by Eqs. 1 and 2 leads to the following expression including just laboratory coordinates that can be applied directly to emittance manipulation scenarios

$$(\varepsilon_1 - \varepsilon_2)^2 + \left[\frac{AB_s}{(B\rho)}\right]^2 + 2\frac{B_s}{(B\rho)}\left[\langle y^2\rangle\langle xy'\rangle - \langle x^2\rangle\langle yx'\rangle + \langle xy\rangle(\langle xx'\rangle - \langle yy'\rangle)\right] = const\,, \tag{9}$$

where $A := \sqrt{\langle x^2\rangle\langle y^2\rangle - \langle xy\rangle^2}$ is the rms-area of the beam divided by π. The last summand (abbreviated as $2\frac{B_s}{(B\rho)}\mathcal{W}_A$) is invariant under rotation around the beam axis and it vanishes for uncorrelated beams. As shown in [6] Eq. (9) is equivalent to

$$(\varepsilon_1 - \varepsilon_2)^2 + \left[\frac{AB_s}{(B\rho)}\right]^2 + \frac{AB_s}{(B\rho)}\oint_C \vec{r}'d\vec{C} = const\,. \tag{10}$$

Emittance reduction through acceleration can be included by multiplying Eqs. (1) and (2) initially by $p = m\gamma\beta c$, where β is the longitudinal particle velocity normalized to the velocity of light c. The extension of Busch's theorem to beams including acceleration is

$$(\varepsilon_{n1} - \varepsilon_{n2})^2 + \left[\frac{eq\psi}{mc}\right]^2 + \frac{eq\psi\beta\gamma}{mc}\oint_C \vec{r}'\cdot d\vec{C} = const\,, \tag{11}$$

where ψ is the magnetic flux through the beam rms-area A. This expression can be further compressed by using the mechanical canonical momentum $\vec{\mathcal{P}}_c = \vec{\mathcal{P}} + eq\vec{\mathcal{A}}$ with $\vec{\mathcal{P}} := m\gamma\vec{v}$ and the canonical vorticity $\vec{\Omega}_c := \vec{\nabla}\times\vec{\mathcal{P}}_c$ to

$$(\varepsilon_{n1} - \varepsilon_{n2})^2 + \frac{eq\psi}{(mc)^2}\int_A \vec{\Omega}_c d\vec{A} = const\,. \tag{12}$$

FLAT BEAM EXPERIMENT AT FERMILAB

At FERMILAB's NICADD photoinjector, flat electron beams were formed by first producing the beams at the surface of a photo cathode placed inside an rf-gun to which longitudinal magnetic field $B_s = B_0$ was imposed [7]. The schematic beam line is sketched in Fig. 2. Along the subsequent region with $B_s = 0$, the beam was accelerated to

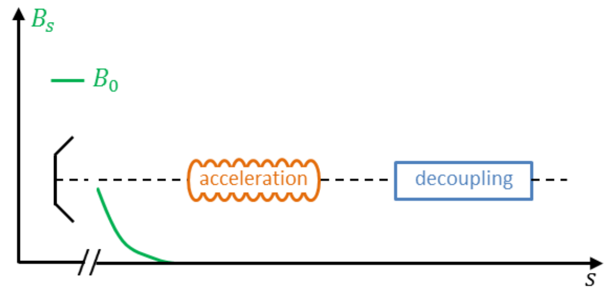

Figure 2: Fig. 6 from [3]: schematic sketch of the beam line of the experiment performed at NICCAD at FERMILAB [7].

16 MeV. Finally, correlations initially imposed by the magnetic exit fringe field of the rf-gun were removed by three skew quadrupole magnets. Equation (11) equalizes the situation at the cathode surface at the left-hand side to the situation of the finally flat beam on the right-hand side ($q = 1$)

$$0 + \left[\frac{eB_0A_0}{mc}\right]^2 + 0 = (\varepsilon_{nf1} - \varepsilon_{nf2})^2 + 0 + 0\,, \tag{13}$$

where A_0 is the beam rms-area at the cathode surface. The authors of [7] used the definitions [8]

$$(\varepsilon_n^u)^2 := \varepsilon_{nf1}\cdot\varepsilon_{nf2} \tag{14}$$

$$\mathcal{L} := (eB_0A_0)/(2m\gamma\beta c) \tag{15}$$

resulting in

$$\varepsilon_{nf1} = \mathcal{L}\beta\gamma \pm \sqrt{(\mathcal{L}\beta\gamma)^2 + (\varepsilon_n^u)^2}\,, \tag{16}$$

of which only the upper sign gives a meaningful positive result. Re-plugging this expression for ε_{nf1} into Eq. (13) leads to

$$\varepsilon_{nf1/2} = \pm\mathcal{L}\beta\gamma + \sqrt{(\mathcal{L}\beta\gamma)^2 + (\varepsilon_n^u)^2}\,, \tag{17}$$

being identical to their original expression (Eq. (1) of [7]).

TRANSVERSE EMITTANCE TRANSFER EXPERIMENT AT GSI

At GSI, the EMittance Transfer EXperiment (EMTEX) transferred emittance from one transverse plane into the other one by passing the beam through a short solenoid [5,9]. The schematic EMTEX beam line is depicted in Fig. 3. In the solenoid center, the ions charge state, i.e., their rigidity was changed by placing a thin carbon foil therein from $^{14}N^{3+}$ to $^{14}N^{7+}$. Charge state stripping is a standard procedure used at several laboratories that deliver heavy or intermediate mass ions [10]. In front of the solenoid, the beam had no inter-plane correlations, and thus, the difference of rms-emittances was equal to the difference of eigen-emittances (mod. sign). Since the solenoid was short, the beam area at the foil $A := A_f$ can be approximated as constant during the beam transit through the solenoid. Table 1 lists the relevant parameters of the experiment. Equation (9)

ISBN: 978-3-95450-194-6 doi:10.18429/JACoW-LINAC2018-TUPO078

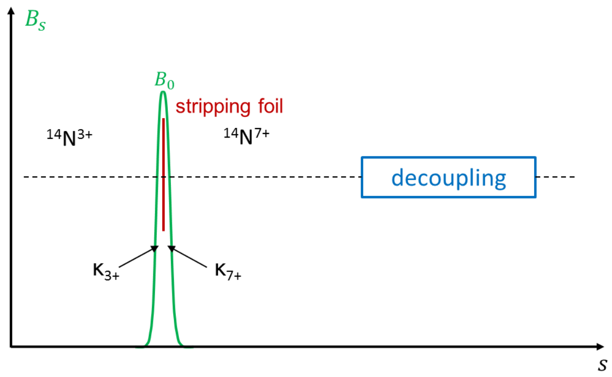

Figure 3: Fig. 7 from [3]: schematic beam line of EMTEX at GSI for transverse emittance transfer [9].

relates the beam parameters in front of the solenoid ($B_s = 0$, no correlations $\rightarrow \mathcal{W}_A = 0$, $\varepsilon_{10} = \varepsilon_{x,3+}$, $\varepsilon_{20} = \varepsilon_{y,3+}$) to those in front of the foil in the center of the short solenoid:

$$(\varepsilon_{x,3+} - \varepsilon_{y,3+})^2 + 0 + 0 = (\varepsilon_{1f} - \varepsilon_{2f})^2 + \left[\frac{A_f B_0}{(B\rho)_{3+}}\right]^2 + \frac{2B_0}{(B\rho)_{3+}}\mathcal{W}_{Af}\,, \tag{18}$$

where the index f refers to the location of the foil. The entrance fringe field of the solenoid causes the rms-vorticity

$$\mathcal{W}_{A_f} = \Delta\mathcal{W}_A = -2\kappa_{3+} \cdot A_f^2 = -2\frac{B_0}{2(B\rho)_{3+}}A_f^2 \tag{19}$$

leading to

$$(\varepsilon_{x,3+}-\varepsilon_{y,3+})^2 + 0 + 0 = (\varepsilon_{1f}-\varepsilon_{2f})^2 - \left[\frac{A_f B_0}{(B\rho)_{3+}}\right]^2 . \tag{20}$$

Using the initial beam parameters of the experiment from Table 1, $A_f = \sqrt{\varepsilon_x\beta_x\varepsilon_y\beta_y} = 4.166\,\text{mm}^2$, and the identity 1 mm mrad = 1 μm gives

$$(\varepsilon_{1f} - \varepsilon_{2f})^2 = (\varepsilon_{x,3+} - \varepsilon_{y,3+})^2 + 2.709\ \mu\text{m}^2 = 2.755\ \mu\text{m}^2\,. \tag{21}$$

Equation (9) is re-used to relate the beam parameters just behind the foil but still at the center of the solenoid to those at the exit of the beam line, where $B_s = 0$ and the beam correlations have been removed again. Angular scattering in the foil is neglected. As the beam changed rigidity in the foil, $(B\rho)_{3+}$ must be properly replaced by $(B\rho)_{7+}$. However, second beam moments are not changed by the foil, i.e., $\mathcal{W}_A = \mathcal{W}_{A_f}$, right in front and right behind the foil. Accordingly,

$$(\varepsilon_{1f} - \varepsilon_{2f})^2 + \left[\frac{A_f B_s}{(B\rho)_{7+}}\right]^2 + \frac{2B_s}{(B\rho)_{7+}}\mathcal{W}_{Af} = (\varepsilon_{x,7+} - \varepsilon_{y,7+})^2 + 0 + 0\,, \tag{22}$$

which by using Eq. (19) and plugging in the values delivers

$$|\varepsilon_{x,7+} - \varepsilon_{y,7+}| = 2.2\ \text{mm mrad} \tag{23}$$

Table 1: EMTEX Beam Parameters

Parameter	Value
kin. energy	11.45 MeV/u
mass number	14
$\varepsilon_{x,3+}$	1.040 mm mrad
$\varepsilon_{y,3+}$	0.825 mm mrad
$\beta_{x,3+}$	3.461 m
$\beta_{y,3+}$	5.845 m
$q_{in/out}$	3+ / 7+
$(B\rho)_{3+/7+}$	2.278 / 0.976 Tm
B_0	0.9 T

fitting well the measured value of 2.0 mm mrad (see Fig. 2 of [9]).

REFERENCES

[1] H. Busch, "Berechnung der Bahn von Kathodenstrahlen im axialsymmetrischen elektromagnetischen Felde", *Annalen der Physik*, vol. 81, pp. 974, (1926).

[2] P. T. Kirstein *et al.*, *Space Charge Flow*. New York, USA: McGraw-Hill Inc., 1967, pp. 14.

[3] L. Groening *et al.*, "Extension of Busch's theorem to particle beams", *Phys. Rev. ST Accel. Beams*, vol. 21, pp. 014201 (2018), doi:10.1103/PhysRevAccelBeams.21.014201

[4] A. J. Dragt, "General moment invariants for linear Hamiltonian systems", *Phys. Rev.* A, vol. 45, no. 4, pp. 2572 (1992), doi:10.1103/PhysRevA.45.2572

[5] C. Xiao *et al.*, "Single-knob beam line for transverse emittance partitioning", *Phys. Rev. ST Accel. Beams*, vol. 16, pp. 044201 (2013), doi:10.1103/PhysRevSTAB.16.044201

[6] L. Groening *et al.*, "Relation between particle beam eigen-emittances and canonical vorticity flux", *arXiv*, 1808.01218 (2018).

[7] P. Piot *et al.*, "Photoinjector generation of a flat electron beam with transverse emittance ratio of 100", *Phys. Rev. ST Accel. Beams*, vol. 9, pp. 031001 (2006), doi:10.1103/PhysRevSTAB.9.031001

[8] K.-J. Kim, "Round-to-flat transformation of angular-momentum-dominated beams", *Phys. Rev. ST Accel. Beams*, vol. 6, pp. 104002 (2003), doi:10.1103/PhysRevSTAB.6.104002

[9] L. Groening *et al.*, "Experimental Proof of Adjustable Single-Knob Ion Beam Emittance Partitioning", *Phys. Rev. Lett.*, vol. 113, pp. 264802 (2014), doi:10.1103/PhysRevLett.113.264802

[10] P. Scharrer *et al.*, "Measurements of charge state distributions of 0.74 and 1.4 MeV/u heavy ions passing through dilute gases", *Phys. Rev. Accel. Beams*, vol. 20, pp. 043503 (2017), doi:10.1103/PhysRevAccelBeams.20.043503